

Inversion of gravity data for base salt

Dongjie Cheng^{*†}, Yaoguo Li^{††}, and Ken Lerner[†],

[†] Center for Wave Phenomena, Colorado School of Mines, Golden, Co

^{††} Gravity and Magnetics Research Consortium, Colorado School of Mines, Golden, Co

Summary

We develop an algorithm for inverting gravity data to construct estimates of the base of salt and investigate the sensitivity of the recovered model to four different sources of errors. The inversion algorithm is based on the approach of Tikhonov regularization. The prior information is typically shape and depth of the top salt and of a known part of base salt from seismic image. The error in such prior information governs the reliability of the recovered base of salt. It is therefore important to understand the influencing factors of the inversion: (1) input gravity data, (2) top of salt, (3) known part of the base salt, and (4) the background density profile. We use a synthetic model to illustrate the algorithm and find that the recovered model can be a good representation of the true model in the absence of errors. Moderate perturbation in any of these four factors could lead to large errors in the recovered model, leaving open the question as when gravity data can aid in improving the image of base salt.

Introduction

Determination of the shape of the base of salt is important in subsalt exploration. Where seismic method alone fails to provide an adequate image of the base of salt, gravity data can potentially complement the seismic data. Previous researchers have developed practical methods for inverting gravity data to construct the base of salt (e.g., Jorgensen *et al.*, 2000). With the increased application of such methods, it is important to understand the factors that influence the final inversion result, in addition to commonly considered issues such as data quality and details of the inversion formulation. We seek to address this issue from a practical point of view by examining the consequence of errors in a set of assumed parameters commonly used in inversions.

To achieve our goal, we first present an inversion algorithm that uses the vertical gravity anomaly as data and inverts for the base of salt by Tikhonov regularization. The model in the inversion is the surface defining the base of salt, and we introduce a logarithmic function to represent it.

Using this algorithm, we investigate the influence of four major factors on the inversion result. In most inversion algorithms, the top of the salt and a part of the base of salt are assumed to be well imaged by seismic. Also, the background sedimentary density, and thus the density contrast of the salt body, are assumed to be known.

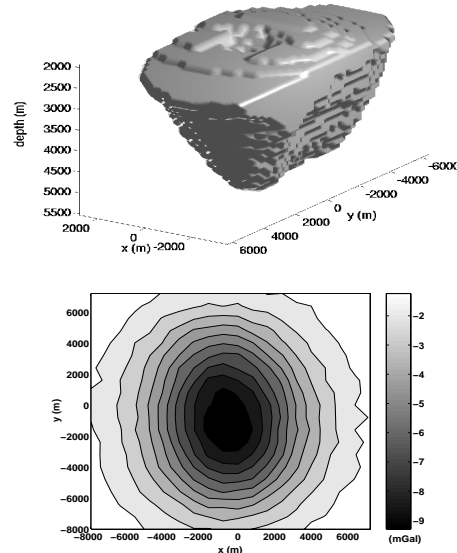


Fig. 1: Synthetic salt model used in the numerical example. The top panel shows a 3D view of the salt model. The staircase appearance reflects the model discretization used in the inversion. The bottom panel is simulated gravity data contaminated with Gaussian noise whose standard deviation is 0.1 mGal.

Furthermore, it is assumed that the gravity data are processed to remove any factors unrelated to the variation in base salt. In practice, however, these assumptions will invariably have errors that have implications for the inversion result. Here, we assess their influence by carrying out simulations assuming different types of errors and empirically quantifying the corresponding uncertainty in the inverted model.

Inversion algorithm

Let $d_i = g_z(x_i, y_i)$, $i = 1, \dots, N$ be the vertical gravity anomaly, $h_t(x, y)$ and $h(x, y)$ be respectively the top and base of the salt body, and $\Delta\rho(z)$ the density contrast between salt and the sedimentary host. We assume that $h_t(x, y)$ and $\Delta\rho(z)$ are known. We also assume that part of $h(x, y)$ may be known and can be incorporated as a constraint in the inversion. The inverse problem is then to construct an estimate of the unknown portion of the $h(x, y)$ using the gravity anomaly and above known information.

We first define a new function to be used as the model in

Gravity inversion for base salt

the inversion:

$$m(x, y) = \ln[h(x, y) - h_t(x, y)]. \quad (1)$$

With this parameterization, the base of salt is given by $h(x, y) = e^{m(x, y)} + h_t(x, y)$. Working with this transformed model ensures the natural condition that the recovered base of salt lies below the top salt. No additional bounding constraint is needed.

We formulate the inversion using Tikhonov regularization and obtain the inverse solution by minimizing

$$\phi = \phi_d + \beta\phi_m, \quad (2)$$

where ϕ_d is the data misfit, ϕ_m is the model objective function, and β is the regularization parameter. The data misfit is defined as,

$$\phi_d = \|W_d(\vec{d} - \vec{d}_{obs})\|_2^2, \quad (3)$$

where \vec{d} is the vector of predicted data, \vec{d}_{obs} contains the observations, W_d is a diagonal data-weighting matrix, whose elements are the inverse of estimated data standard derivations. The model objective function is defined to penalize the length and structural complexity of the model to be recovered. We can also incorporate a reference model m_0 , which can be formed from the estimates of base salt derived from seismic imaging.

To perform numerical computation, we discretize both top and base of salt into piece-wise constant surfaces defined over a common set of contiguous rectangular cells within the area over which the base salt is defined. Such a discretization divides the salt body into a set of contiguous vertical prisms. The unknown model is represented as a vector, $\vec{m} = (m_1, \dots, m_M)^T$, where M is the number of cells. The discretized objective function is then expressed as

$$\phi = \|W_d(\vec{d} - \vec{d}_{obs})\|_2^2 + \beta\|W(\vec{m} - \vec{m}_0)\|_2^2, \quad (4)$$

where W is the discretized operator of the model objective function.

Since the gravity data on the surface is nonlinearly related to the model \vec{m} , the minimization of eq.(4) is a nonlinear process. We use the standard Gauss-Newton method to obtain the solution. Let $\vec{m}^{(k)}$ be the model recovered at the k th iteration, and $\vec{d}^{(k)}$ be the corresponding predicted data. The model perturbation $\delta\vec{m}^{(k+1)}$ for the $(k+1)$ th iteration is given by the equation,

$$(G^T W_d^T W_d G + \beta W^T W) \delta\vec{m}^{(k+1)} = [W_d^T G^T W_d (\vec{d}_{obs} - \vec{d}^{(k)}) + \beta W^T W (\vec{m}_0 - \vec{m}^{(k)})], \quad (5)$$

where G is the sensitivity matrix evaluated at the model $\vec{m}^{(k)}$. The updated model for $(k+1)$ th iteration is given by

$$\vec{m}^{(k+1)} = \vec{m}^{(k)} + \alpha \delta\vec{m}^{(k+1)}, \quad (6)$$

where $0 < \alpha \leq 1$ is a chosen step length. The corresponding depth of base of salt is given by

$$h_j^{(k+1)} = h_{tj} + e^{m_j^{(k+1)}}, \quad j = 1, \dots, M. \quad (7)$$

This base of salt is then used to calculate the predicted data for the $(k+1)$ th iteration, and the inversion proceeds to the next iteration. The process continues until the objective function converges.

As in any regularized inversion, the choice of regularization parameter is crucial. Because of the long list of processing steps applied to the data and because the residual geological noise, such as bathymetry error, is often present in the data, the data errors are commonly correlated with the noise. In addition, we seldom have knowledge about the precise statistics of these errors. For these two reasons, we opt to using the L-curve criterion (Hansen, 1992) to estimate the optimal value of β .

Numerical example

We use the synthetic salt model shown in the top panel in Figure 1 to illustrate the performance of the algorithm and to carry out simulations for estimating the uncertainties in the recovered model in the next section. The model is assumed to lie below the ‘nil-zone’; therefore the salt body has negative density contrasts that increase in magnitude with depth. With the top and the base of salt discretized into 250-m square cells, we generate 400 observations and contaminate them with Gaussian random noise having a standard deviation of 0.1 mGal to simulate observed data. These data are shown in gray-scale contours in the bottom panel Figure 1.

To emulate real situations, we assume that the part of the base of salt shown by the gray contours in Figure 2 is known. We fix this part during the inversion, and the unknown model to be recovered is defined over the central region in Figure 2. The base of the salt in the reference model has a 4000-m constant depth and the maximum difference between the true and the reference model is 1500 m. Figure 3 shows a comparison between the true and recovered model. The latter is a good representation of the true model (Figure 4), with an root-mean-square (RMS) difference of 169 m between the two.

For the current example, this can be considered the best model from the inversion since all the assumptions are correct. Using this model as the basis for comparison, in the next section we proceed to evaluate the sensitivity of inverted base of salt to different sources of error.

Sensitivity study

The inverted model is strongly dependent on errors in four types of input data: (1) gravity data, (2) high-confidence zone, (3) top of salt, and (4) background density profile. It is of practical importance to gain quantitative understanding of the errors in the inverted model that could be produced by a given level of errors

Gravity inversion for base salt

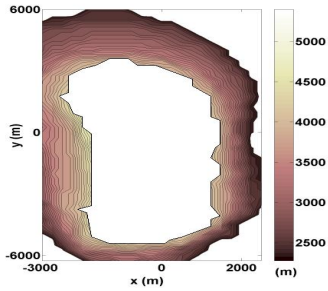


Fig. 2: Plan view in which the contoured region shows the known portion of the base of salt while the blank region in the center is the area of unknown base of salt to be recovered from the inversion. The region of known base of salt is termed the *high-confidence zone* (HCZ).

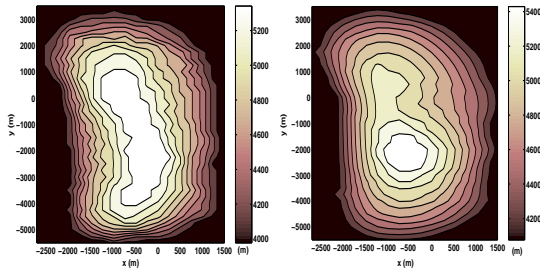


Fig. 3: Comparison between the depths of the true base of salt (a) and those of the recovered model (b).

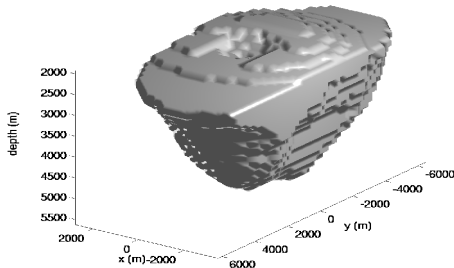


Fig. 4: 3D view of the recovered model. Compare with the structure of the true model in Figure 1.

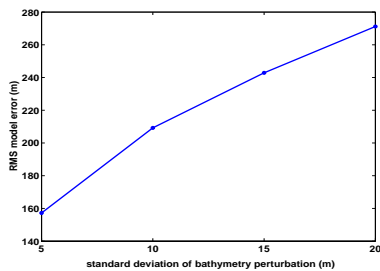


Fig. 5: RMS difference between the recovered and true base of salt as a function of geological noise. The noise is introduced by a variable bathymetry simulated using a correlated random perturbation with different standard deviations.

in these input parameters. In this section, we carry out four sets of inversions by introducing different levels of error in one parameter while using the correct input for the remaining three. The error in the recovered model is measured by the RMS difference from the true model (for the data error) or from the best inversion result in the absence of errors (for the other three factors).

Data error It is a common practice, although not realistic, to simulate data error by using uncorrelated random noise. In addition, since no geologically reasonable base-salt structure at a depth of several km can produce highly variable gravity anomalies on the surface, results from our algorithm using the L-curve criterion do not change dramatically in the presence of such noise. We therefore choose to focus on one type of noise that can often occur in practical applications: the data error caused by inaccurate bathymetry correction.

We emulate its influence by adding to the data in Figure 1 the gravity anomaly produced by correlated random perturbations to the bathymetry. The random perturbation has a Gaussian autocorrelation function with a correlation length of 400 m. We use four different standard deviations for the perturbation: 5, 10, 15 and 20 m. The correct bathymetry is assumed to be a constant at the depth of 1200 m. For each simulation, we compute the gravity anomaly attributed to the bathymetry perturbation, add it to the data, and invert the contaminated data to construct the base salt. The RMS difference between the recovered and true base of salt, shown in Figure 5, increases monotonically with the amplitude of the perturbation. With a 10-m perturbation, for example, the RMS difference exceeds 200 m.

Error in high-confidence zone In practice, one often fixes a portion of the base of salt in the inversion that is believed to accurately known. This part of the base of salt is called the *high confidence zone* (HCZ). Correct specification of the HCZ can help the inversion since it provides an additional constraint. If the HCZ is incorrectly defined, however, it can greatly degrade the result and produce large errors. We assess the sensitivity of the recovered model to errors in the specified HCZ by perturbing it by $\pm 2.5\%$, $\pm 5\%$ and $\pm 10\%$ from the true depth and then carrying out the inversions and comparing the results with the best model shown in Figure 3.

As one might expect, the recovered models move in the opposite direction as the HCZ is perturbed up or down. The influence of error in HCZ is dramatic: a 5% perturbation produces a maximum difference of more than 1000 m, as illustrated in Figure 6. Figure 7 displays the RMS difference between the best model and the models recovered with incorrect HCZ. These results suggest that one should not simply fix the HCZ in the inversion unless it is known accurately. A reference model is then appropriate for incorporating an HCZ.

Error in top salt In seismic imaging, the velocity error in shallow regions can cause at the least a DC shift in depth of the base salt image. We simulate this error by perturbing the top salt by a constant, moving

Gravity inversion for base salt

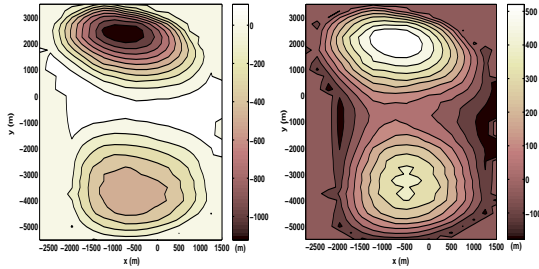


Fig. 6: Difference between the depth of base salt from the best model and a model that used an incorrect HCZ. The two panels show the results when the HCZ is moved up (left) and down (right) by 5%, which translates to a maximum perturbation of 270 m. The maximum error exceeds 1000 m.

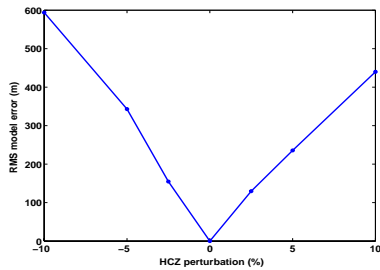


Fig. 7: RMS depth difference between the best model and models using incorrect HCZ.

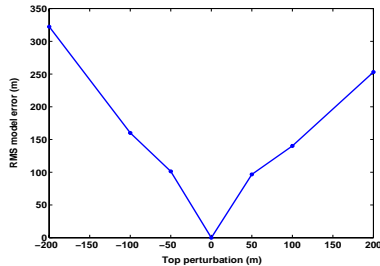


Fig. 8: RMS depth difference between the best model and models with incorrect top salt.

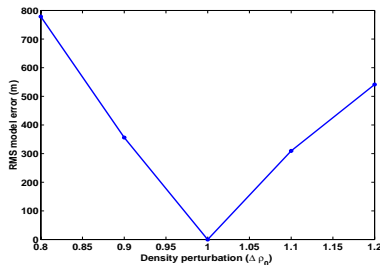


Fig. 9: RMS depth difference between the best model and models with incorrect density contrast. $\Delta \rho_0$ is the correct density contrast.

the known salt up or down in depth while preserving its shape. Specifically, we perturb the depth of top salt by ± 50 , ± 100 and ± 200 m, respectively. The model loses the *keel-shaped* feature when the salt is shifted up and extends the keel deeper when the salt moved downward. In addition, a constant error in top salt introduces complex structure into the recovered base salt, which can lead to erroneous interpretation and degrade seismic imaging of the section beneath the salt. The RMS differences for all perturbations are summarized in Figure 8.

Error in density contrast The background density in the sedimentary host is typically obtained from the density logs in sparsely located wells in the general vicinity of the salt body. A single density profile is often used throughout the entire 3D model region, and even where a laterally variable background density volume is constructed it may not be an accurate enough representation. We carry out a sequence of simple simulations by perturbing the density contrast by $\pm 10\%$ and $\pm 20\%$. The influence of error in the density contrast is relative simple. The depth of the base of salt increases as the density contrast decreases, but no complex structure is introduced. Figure 9 shows the RMS difference as a function of the density contrast. A 10% error in density contrast leads to an RMS error of about 300 m.

Discussion

Using our newly developed algorithm, we have carried out quantitative studies to assess the errors in the inverted base of salt produced by the four factors as mentioned above. Seemingly small errors in these input parameters can lead to significant errors in the recovered base salt. Thus one must minimize errors in these input parameters in order for them to improve the reliability of the inverted base of salt. Our derived error curves provide an indication of errors to be expected in the inverted base of salt in practical applications, and serve as a guide to data preparation so that the inverted base salt can aid in seismic imaging of base salt and, thereby, the subsalt structure.

Acknowledgment

We thank the industry sponsors of the consortia Center for Wave Phenomena (CWP) and Gravity and Magnetics Research Consortium (GMRC) for their support.

References

- Hansen, P., 1992, Analysis of discrete ill-posed problems by means of the L-curve: 69th SIAM Review, 34, 561-580.
- Jorgensen, G. and Kisabeth, J., 2000, Joint 3-D inversion of gravity, magnetic, and tensor gravity fields for imaging salt formations in the deepwater Gulf of Mexico, 70th Ann. Internat. Mtg: Soc. of Expl. Geophys., 424-426.